High resolution visualization of acoustic wave fields within surface acoustic wave devices

T. Hesjedal,[a] E. Chilla, and H.-J. Fröhlich
Paul-Drude-Institut für Festkörperelektronik, D-10117 Berlin, Germany

(Received 5 November 1996; accepted for publication 10 January 1997)

We present the submicron visualization of surface acoustic wave (SAW) fields within interdigital transducers (IDTs) obtained by a scanning acoustic force microscope. Utilizing the nonlinear force curve of the tip-to-surface interaction, a periodic deflection of the cantilever appears when the SAWs are excited intermittently. This deflection depends on the amplitude of the surface oscillation and was measured by lock-in technique. SAWs with operating frequencies above 600 MHz were detected. The influence of the mass loading on the local oscillation amplitude was studied for various layer thicknesses of the IDT electrodes. © *1997 American Institute of Physics.* [S0003-6951(97)01711-7]

Among the various methods for the detection of surface acoustic waves (SAWs), like voltage-contrast scanning electron microscopy,[1,2] laser optical[3–6] and capacitive[7] probing, holographic techniques,[8] and stroboscopic x-ray topography techniques,[9,10] the first two methods practically offer the highest lateral resolution and were utilized for the mapping of acoustic wave fields within SAW devices. The scanning electron microscopy visualization of SAW excitation was first achieved on a 36 MHz interdigital transducer (IDT).[11] Thereby, the spatial resolution is limited to about 1 μm as a consequence of the charging of the piezoelectric substrate and the subsequent image distortion. Furthermore, this method is limited in SAW frequency to the lower MHz range as it needs a high voltage chopper. Laser optical probing has been applied for the first time for 105 MHz IDTs achieving a lateral resolution of 20 μm.[12] However, the method's lateral resolution limit is determined by Abbe's criteria. Both methods are highly sensitive to changes of the conductivity and reflectivity of the surface, respectively. In particular, the partially metal-covered surface areas within the IDT have a large impact on the image resolution.

With the demand of GHz SAW devices for mobile communication the structural length of the IDTs will meet the submicron scale. Although the device design has reached the GHz frontier with conventional IDT modeling, second order effects caused by SAW diffraction, electrode edges, propagation losses due to scattering at surface inhomogeneities, and mass loading play an increasing role in the higher frequency range.

Consequently, submicron SAW devices demand new diagnostic techniques. The invention of scanning probe methods with their resolution down to the atomic scale has opened up new ways for SAW investigations. Recently, a scanning tunneling microscopy technique for mapping amplitude and phase of acoustic waves on conducting samples under ambient conditions was presented.[13] SAWs were also detected on nonconducting samples by using a scanning force microscope (SFM).[14] Since typical SFM cantilever resonance frequencies are up to some 100 kHz, a cantilever cannot follow the high frequency surface oscillations induced by SAWs. Nevertheless, due to the nonlinear force-to-distance dependence the normal component of the wave amplitude affects an additional static deflection of the cantilever. This shift is caused by the time average of the surface oscillation and nonlinear interaction.[15] Various high frequency signals can be determined by employing the nonlinear force behavior in the sense of a mixer. Electrical mixing has been used to measure the electrical charge distribution on IDT electrodes.[16] The mixing of two SAWs has been applied for the determination of the acoustic phase velocity on the nanometer scale.[17]

Here we report on the first visualization of the amplitude of SAWs within an IDT by a scanning acoustic force microscope (SAFM)[18] with submicron lateral resolution. The local effect of mass loading by the thickness variation of the IDT fingers is discussed.

The investigated single finger IDT with 500 acoustic sources was fabricated on ST-quartz with SAW propagation parallel to the X axis (Euler angles: 0°, 132.75°, 0°). The operating frequency was 602.7 MHz. The 1.3 μm spaced Al electrodes of the different IDTs had thicknesses of 86 nm and 110 nm, respectively. The acoustic wavelength was $\lambda = 5.2$ μm and the transducer's aperture formed by the overlapping Al fingers was 5 λ. To avoid the influence of reflected SAWs from substrate edges they were covered with an acoustic absorber. The experiments were performed in air and at room temperature using a modified LS autoprobe™ SFM. The rf generator signal output fed to the IDT without any electrical matching was less than 10 dBm and was sinusoidally amplitude modulated at a low frequency between 5 and 50 kHz. This modulation frequency was used as the reference frequency of a lock-in amplifier to analyze the low-frequency component of the cantilever deflection signal. The scan frequencies ranged from 2 Hz for preview scans down to 0.2 Hz for detailed measurements. The cantilevers had a thickness of 1.8 μm, a stiffness of 1.9 and 18 N/m, and a resonance frequency of 50 and 350 kHz, respectively. The measurements were performed in contact mode in order to obtain the pure acoustic contributions to the deflection signal and to avoid surface charge effects.[16]

Figure 1 shows a 60×30 μm^2 SAFM image of an IDT with 86 nm thick Al electrodes. In the topographical image [Fig. 1(a)] the collector electrodes are clearly visible on the left- and the right-hand side of the device. The electrode

[a]Electronic mail : hesjedal@pdi.wias-berlin.de

 0003-6951/97/70(11)/1372/3/$10.00

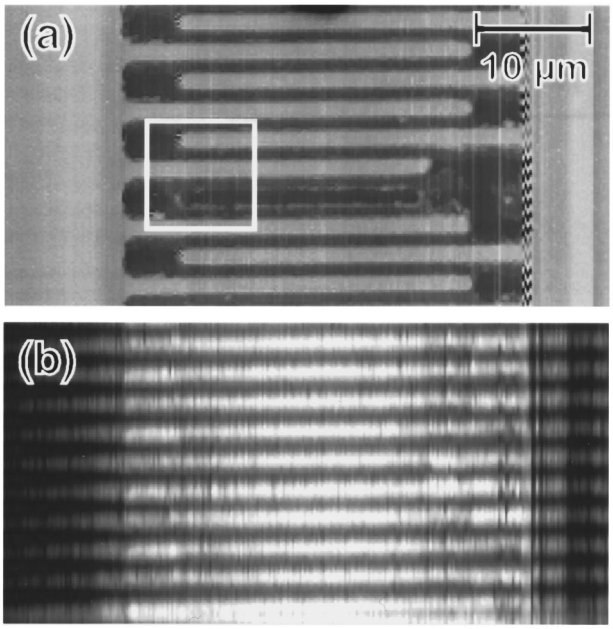

FIG. 1. (a) Topographical image and (b) surface oscillation amplitude of a 60×30 μm^2 SAFM scan. The IDT consists of 86 nm thick Al electrodes on ST-X quartz. The operating frequency was 602.7 MHz. The acoustic wavelength was $\lambda=5.2$ μm and the width of the Al fingers was $\lambda/4$.

fingers are oriented horizontally. Two neighboring fingers form an acoustic source. At the center of the image an electrode finger has been removed to study the influence of a defect on the IDT performance. Figure 1(b) shows the surface oscillation which was measured simultaneously with the topography. A periodicity of $\lambda/2$ can be observed. This standing wave pattern is caused by phase synchronous interference of the waves launched in the opposite directions. The nodes and antinodes are oriented parallel to the fingers and are revealed as dark and light areas, respectively. The oscillation amplitude is decaying towards the collector electrodes. Although the IDT has a remarkable local damage, there is almost no influence on its dynamic behavior, i.e., the wave pattern appears unchanged.

Figure 2 shows the zoom of the rectangular area marked in Fig. 1(a). The position of the node pattern with respect to the metal electrodes marked by solid lines is revealing the crystal symmetry of the substrate. For ST cut quartz with X propagation direction the phase between the displacement component normal to the surface and the electrical potential is 90°.[19] As the electrical potential distribution is determined by the position of the electrodes the acoustic maxima are placed between the fingers. The dashed line marks the missing electrode. The oscillation signal is a little higher for the free surface where the electrode is missing compared with the equivalent metal covered area at the top of the image. When increasing the electrode thickness the influence of the mass loading also increases. Figure 3 shows a SAFM image of an IDT with 110 nm thick Al electrodes. The removal of the electrode finger which can be found in the center of Fig. 3(a) has a much larger impact on the oscillation amplitude pattern [Fig. 3(b)] than for the thinner electrodes. Now, at the position of the missing finger, a bright bar is evident. Also in the metal free area between the finger ends and the collector electrodes remarkably bright maxima are visible. However,

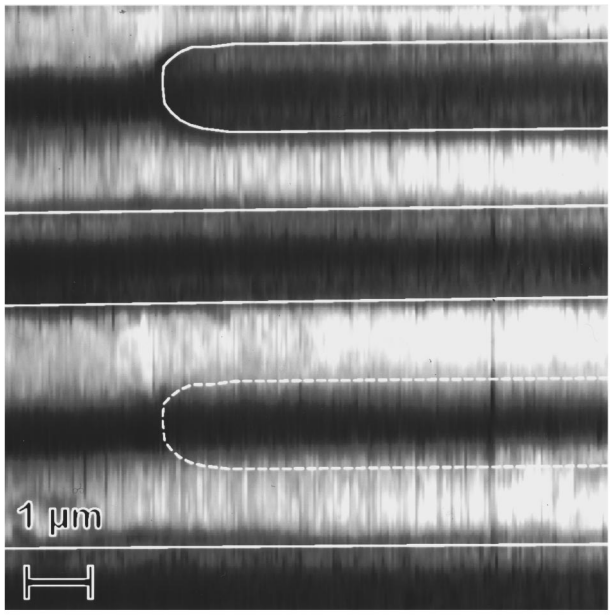

FIG. 2. Oscillation amplitude measured over 10×10 μm^2 [zoom of Fig. 1(a)] within 86 nm thick IDT electrodes. The solid lines represent the Al fingers. The position of the missing finger is marked by the dashed line.

where the crystal symmetry is concerned two bright features should appear at the position of the missing finger as well as at the finger ends. Figure 4 shows a detailed scan as indicated by the square in Fig. 3(a). There it can be seen that the amplitude pattern is slightly shifted compared with the crystal symmetry prediction determined by the electrode arrangement. As a consequence the antinodes move slightly towards the electrodes and therefore one of the antinodes is damped stronger than the other. This shifting cannot be observed for the thin electrodes, i.e., that mass loading can have an influence on the node pattern position particularly when the measurement area is far from the center of the IDT. Different

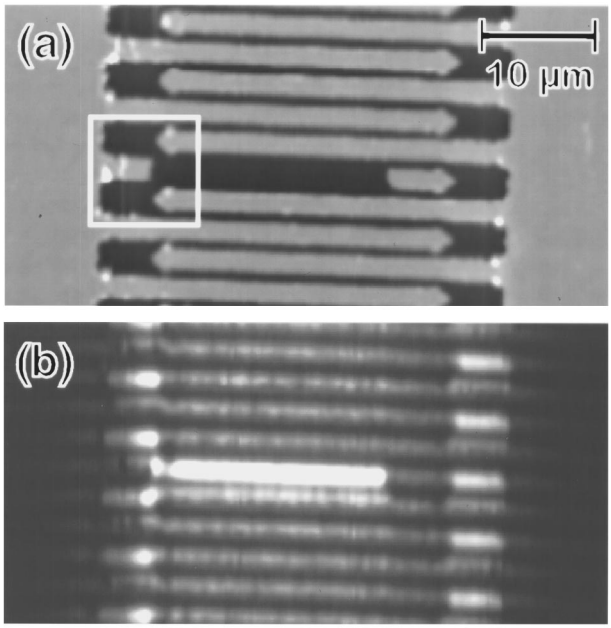

FIG. 3. (a) Representation of the topography and (b) the oscillation amplitude of 110 nm thick Al electrodes acquired over 60×30 μm^2. A large increase of the signal appears when an electrode is missing.

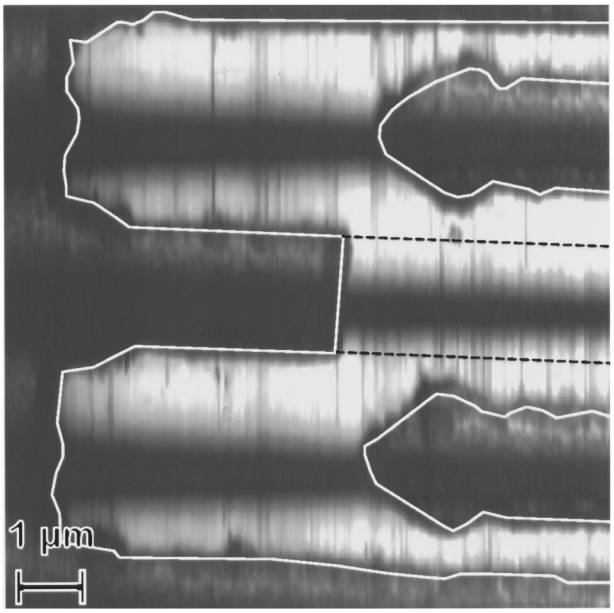

FIG. 4. 10×10 μm^2 detail scans [square in Fig. 3(a)] of the oscillation amplitude. The oscillation amplitude pattern is shifted with respect to the electrodes.

electrode thicknesses can change the acoustic properties of the IDT. As a result, the confinement of the oscillation node pattern to the electrode pattern varies when changing the layer thickness and the operating frequency, respectively. This is in agreement with SAW delay line transmission measurements. By analyzing this transmission between two IDTs using a network analyzer it can be found that an electrode thickness variation leads to a shift of the center frequency of the pass band.

For the quantitative estimation of the mass loading on the wave propagation the physical processes of the tip-to-surface interaction force must be known in detail. Several sources of artifacts have to be regarded coming from the different physical properties of the mapped electrodes and piezoelectric materials. First, the static cantilever deflection due to the high frequency oscillation of the surface may be influenced by damping effects. Since surface contaminants like adsorbates and water are material dependent ultrahigh vacuum (UHV) conditions are preferable. Second, the different temperatures of the resistance-heated electrodes and the underlying substrate may lead to undesired site-dependent deflections.[16] Nevertheless, this contribution is about two orders of magnitude smaller than the signal of interest.

In summary, this letter presents a submicron lateral visualization of SAWs within an IDT. Hereby, a modified scanning force microscope setup was used. Amplitude measurements within the IDT reveal the standing wave pattern and the influence of the finger's mass loading. In the future this method could be used to enhance IDT design in the GHz range by measuring the influence of second order effects of SAW propagation. Furthermore, mapping of the wave amplitude on the free propagation path with high lateral resolution will also be useful for high-resolution SAW focusing[20] and self-focusing Rayleigh wave[21] studies at higher SAW frequencies.

[1] P. Hiesinger, *1972 Ultrasonics Symposium Proceedings* (IEEE, New York, 1978), p. 611.
[2] W. J. Tanski and N. D. Wittels, Appl. Phys. Lett. **34**, 537 (1979).
[3] E. P. Ippen, Proc. IEEE **55**, 248 (1967).
[4] A. Korpel, L. J. Laub, and H. C. Sievering, Appl. Phys. Lett. **10**, 295 (1967).
[5] J. Krokstad and L. O. Svaasand, Appl. Phys. Lett. **11**, 155 (1967).
[6] D. C. Auth and W. G. Mayer, J. Appl. Phys. **38**, 5138 (1967).
[7] B. A. Richardson and G. S. Kino, Appl. Phys. Lett. **16**, 82 (1970).
[8] T. Chiba and Y. Togami, Appl. Phys. Lett. **29**, 793 (1976).
[9] R. W. Whatmore, P. A. Goddard, B. K. Tanner, and G. F. Clark, Nature (London) **299**, 44 (1982).
[10] R. W. Whatmore, P. A. Goddard, and B. K. Tanner, *1982 Ultrasonics Symposium Procedings* (IEEE, New York, 1982), p. 363.
[11] G. Eberharter and H. P. Feuerbaum, Appl. Phys. Lett. **37**, 698 (1980).
[12] P. J. Vella and G. I. A. Stegeman, Appl. Phys. Lett. **22**, 480 (1973).
[13] W. Rohrbeck, E. Chilla, H.-J. Fröhlich, and J. Riedel, Appl. Phys. A **52**, 344 (1991); E. Chilla, W. Rohrbeck, H.-J. Fröhlich, R. Koch, and K. H. Rieder, Appl. Phys. Lett. **61**, 3107 (1992); T. Hesjedal, E. Chilla, and H.-J. Fröhlich, *ibid.* **69**, 354 (1996).
[14] W. Rohrbeck and E. Chilla, Phys. Status Solidi A **131,** 69 (1992).
[15] O. Kolosov and K. Yamanaka, Jpn. J. Appl. Phys. **32**, L1095 (1993).
[16] T. Hesjedal, E. Chilla, and H.-J. Fröhlich, Appl. Phys. A 61, 237 (1995).
[17] E. Chilla, T. Hesjedal, and H.-J. Fröhlich (unpublished).
[18] E. Chilla, T. Hesjedal, and H.-J. Fröhlich, *1994 Ultrasonics Symposium Proceedings* (IEEE, New York, 1994), p. 363.
[19] G. Martin, M. Weihnacht, and K. Franke, IEEE Trans. Ultrason. Ferroelectr. Freq. Control **UFFC-41,** 646 (1996).
[20] R. E. Vines, Shin-ichiro Tamura, and J. P. Wolfe, Phys. Rev. Lett. **74**, 2729 (1995).
[21] R. K. Ing, M. Fink, and O. Casula, Appl. Phys. Lett. **68**, 161 (1996).